Two-dimensional magnetophotonic crystal: Exactly solvable model

A. B. Khanikaev, A. V. Baryshev,* and M. Inoue
Toyohashi University of Technology, Toyohashi, Aichi 441-8580, Japan

A. B. Granovsky and A. P. Vinogradov
Faculty of Physics, Moscow State University, Moscow, Russia
(Received 25 October 2004; revised manuscript received 28 March 2005; published 18 July 2005)

We present an analytical treatment of a two-dimensional (2D) magnetophotonic crystal (MPC) with a square lattice constructed from two infinite arrays of magnetoactive dielectric sheets at right angles, in the limit of very small sheet thickness and very high dielectric constant. Alteration of band structure by an external magnetic field is studied. Two different geometries are examined: the Faraday geometry—magnetic field parallel to the plane of 2D MPC—and the Voigt (Cotton-Mutton) geometry—magnetic field orthogonal to the plane of 2D MPC. In the case of Faraday geometry, we show that the optical activity reduces the symmetry of the system and removes degeneracy in the photonic band structure. Also, despite the weakness of magneto-optic activity, the dispersion $\omega(\mathbf{k})$ near band edges is strongly sensitive to external magnetic influence. In the vicinity of degeneracy, electromagnetic modes exhibit bistable behavior and discontinuously change their dispersion $\omega(\mathbf{k})$ when external magnetic field is applied. In the Voigt geometry *s* and *p* polarizations remain independent of each other, and only the band structure for *s*-polarized light is insignificantly altered.

DOI: 10.1103/PhysRevB.72.035123 PACS number(s): 42.70.Qs, 78.20.Ls, 41.20.Jb

I. INTRODUCTION

The past decade has witnessed a great deal of interest in photonic crystals (PC's) in which the dielectric constituents are periodically arranged.[1,2] These crystals have many interesting properties as far as basic physics is concerned but also in relation to technological applications. The possibility of tuning the properties of PC's such as band structure or dispersion by some external influences may considerably enhance the significance of PC's for applications.

To the best of the authors' knowledge, the tunability of the photonic crystals was originally proposed in Refs. 3 and 4 in which the utilization of external static magnetic or electric fields was suggested for tuning band structure in PC's composed from materials that possess natural magneto-optic activity or tunable anisotropy. Recently the theoretical study of two-dimensional (2D) PC's infiltrated by liquid crystals has also demonstrated the possibility of tuning refraction by rotating the director of liquid crystals.[5] The disappearance of the uncoupled modes[6,7] and splitting of the degenerate branches of the photonic band structure[8] due to symmetry breaking of PC's has also recently been demonstrated. As will be shown below, similar phenomena appear in magnetophotonic crystals (MPC's)—PC's that have at least one constituent material possessing magneto-optic activity.

Further investigation of MPC's has revealed new interesting features and phenomena. For example, in one-dimensional structures, which allow exact analytical treatment by the transfer matrix method, a huge enhancement of the magneto-optic effects was found at the band edges of PC's.[9] In the case of a PC with the introduced magneto-optic defect, the same effect was demonstrated for frequencies corresponding to the eigenmodes localized at the defect.[9]

Recently, using general group-theoretical methods, Figotin and Vitebskiy demonstrated some unusual and interesting behavior of the electromagnetic waves in MPC's.[10,11] They showed that by proper spatial arrangement of magnetic and dielectric components, an MPC with strong spectral asymmetry or nonreciprocity could be constructed. Such MPC's demonstrate unidirectionality—i.e., transparency for electromagnetic modes of the fixed frequency in the specific direction—while modes of the same frequency propagating in the opposite direction have zero group velocity and are completely "frozen."

Work devoted to the theoretical study of two-dimensional MPC's has been presented recently.[12] Using perturbation theory in the vicinity of high-symmetry points of the Brillouin zone, the authors demonstrated enhancement of the Faraday rotation at the band edges and alteration of the band structure.

In the present work we study a MPC model that allows exact analytical study without the aid of perturbative methods. We analyze the behavior of electromagnetic waves inside an artificial 2D MPC formed from magneto-optic dielectric sheets and examine the influence of external magnetic field on photonic band structure.

We develop a generalization of the model originally proposed by Shepherd and co-workers for investigation band structure in 2D PC formed from optically inactive (isotropic) sheets.[13] Recently, a 3D generalization of this model has also been developed and analyzed with aid of analytic perturbation theory.[14] In order to generalize this model to the case of the MPC we rederive it with a dynamical (transfer) matrix approach that allows us to include the influence of magneto-optic activity.

Some may claim that no need exists for artificial and abstract models because we already have powerful numerical methods developed for band structure calculations that allow investigate any properties of PC's. Nevertheless, numerical calculations often serve only to obscure the basic physics, which can be quite simple. Moreover, the electronic Kronig-Penney counterpart of the soluble model developed in Ref.

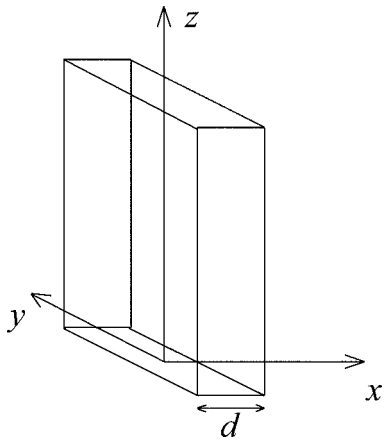

FIG. 1. Geometrical arrangement of a single dielectric slab showing the coordinate axes.

13 was very useful in investigation of band structure of solids[15] and localization of electronic wave functions.[16] Therefore we argue that considering artificial and abstract models is worthy for acquiring insight and physical meaning.

The optical properties of single magnetoactive dielectric sheet, from which the two-dimensional structure is formed, are treated in Sec. II. A one-dimensional lattice of these sheets is considered in Sec. III. The band structure calculations of a two-dimensional MPC and its analysis are presented in Sec. IV. Finally, conclusions are summarized in Sec. V.

II. MAGNETOACTIVE DIELECTRIC SHEET

The elemental block of our artificial model is magnetoactive dielectric sheet of thickness d and relative permittivity ε_L and ε_R for left- and right-polarized light, respectively, taken in the limit

$$d \to 0, \quad \varepsilon_L \to \infty, \quad \text{and } \varepsilon_R \to \infty \text{ such that } \varepsilon_L d \equiv m_L = \text{const and } \varepsilon_R d \equiv m_R = \text{const}. \tag{2.1}$$

For brevity of successive expressions we introduce the additional parameters

$$\varepsilon = \frac{\varepsilon_L + \varepsilon_R}{2}, \tag{2.2}$$

$$\Delta \equiv (\varepsilon_L - \varepsilon_R) d = \text{const, and}$$

$$m \equiv (\varepsilon_L + \varepsilon_R)/2d = \varepsilon d = \text{const}.$$

Parameters m and Δ defined in this way have the dimensions of length: the first defines the averaged optical properties of a single sheet, and the second describes its magnetically induced anisotropy.[17] In the present section, we consider a 4×4 matrix approach[18] in the limit (2.1) to find the transfer matrix of the infinitesimal magnetoactive sheet.

Figure 1 shows the arrangement of a dielectric slab, which was initially assumed to have nonzero thickness d and finite relative permittivity for the left ε_L and right ε_R polarized light. The slab is assumed to have vacuum on either side, but generalization to an arbitrary isotropic background medium with permittivity ε_B by substitutions $m \to m/\varepsilon_B$ and $\Delta \to \Delta/\varepsilon_B$ can be achieved.

First, we consider the processes of reflection and refraction at the surface of semi-infinite dielectric medium. Regardless of the magneto-optic activity of the medium, boundary conditions require continuity of tangential components of electric and magnetic field on the boundary. It is well known that simplification of expressions can be achieved by introducing the 4×4 matrix approach according to which two matrixes $\hat{D}_1$ and $\hat{D}_2$ match the amplitudes of electric fields at two opposite sides of the boundary:

$$\hat{D}_1 \begin{pmatrix} E_s^+ \\ E_s^- \\ E_p^+ \\ E_p^- \end{pmatrix}_1 = \hat{D}_2 \begin{pmatrix} E_s^+ \\ E_s^- \\ E_p^+ \\ E_p^- \end{pmatrix}_2, \tag{2.3}$$

where the superscript $+$ $(-)$ corresponds to the amplitude of wave propagation in the positive (negative) x-axis direction, the subscript s (p) denotes components of a linear polarized electromagnetic wave, and indices 1 and 2 refer to media at opposite sides of the boundary. The dynamical matrix, which matches electric field amplitudes from the left side of the boundary to the right side, can be expressed in terms of Fresnel refraction (t) and reflection (r) coefficients:[18]

$$\hat{D}_{12} = \hat{D}_2^{-1} \times \hat{D}_1 = \begin{bmatrix} 1/t_{12}^s & r_{12}^s/t_{12}^s & 0 & 0 \\ r_{12}^s/t_{12}^s & 1/t_{12}^s & 0 & 0 \\ 0 & 0 & 1/t_{12}^p & 1/t_{12}^p \\ 0 & 0 & r_{12}^p/t_{12}^p & 1/t_{12}^p \end{bmatrix}, \tag{2.4}$$

where indexes "12" at Fresnel coefficients means propagation through the boundary from media with index 1 to media with index 2 and s (p) as before denotes polarization. For completeness we give expressions for Fresnel coefficients here:

$$t_{12}^s = \frac{2k_{1x}}{k_{1x}+k_{2x}}, \quad r_{12}^s = \frac{k_{1x}-k_{2x}}{k_{1x}+k_{2x}},$$

$$t_{12}^p = \frac{2n_1 n_2 k_{1x}}{n_2^2 k_{1x} + n_1^2 k_{2x}}, \quad r_{12}^p = \frac{n_2^2 k_{1x} - n_1^2 k_{2x}}{n_2^2 k_{1x} + n_1^2 k_{2x}}, \tag{2.5}$$

where $n_i = \sqrt{\varepsilon_i}$ is the refractive index of the medium indexed by i and k_{ix} is the projection of the wave vector on the x axis in this medium.

Now we return our attention to the slab of the finite thickness. To allow for the slab's magneto-optic activity, we introduce different propagation velocities for right- and left-polarized light inside of the slab's medium.[17] Consequently, the left- and right-circular-polarized light will gain different phase during propagation through the slab. This effect in the matrix approach can be considered by introducing a propagation matrix that connects the amplitudes of the electric field at different points of the same medium.[18] This matrix in magnetoactive media is diagonal in circular polarization representation and has the following form

$$\hat{P}^{circ} = \begin{bmatrix} e^{ik_L d} & 0 & 0 & 0 \\ 0 & e^{-ik_L d} & 0 & 0 \\ 0 & 0 & e^{ik_R d} & 0 \\ 0 & 0 & 0 & e^{-ik_R d} \end{bmatrix}, \tag{2.6}$$

where $k_{L(R)}=(\omega/c)n_{L(R)}=(\omega/c)\sqrt{\varepsilon_{L(R)}}$ is the absolute value of wave vector in the magnetoactive medium, c is the velocity of light in vacuum, and ω is its frequency.

The final step in studying the magnetoactive infinitesimal dielectric sheet is to construct its transfer matrix in the limit (2.1). Notice that expression (2.6) is given in circular polarization representation, whereas the dynamical matrix (2.4) is given in linear polarization representation. To convert the propagation matrix (2.6), note that from Snell's law $\sin(\theta_2)=(\sqrt{\varepsilon_2}/\sqrt{\varepsilon_1})\sin(\theta_1)$ when the slab permittivity tends to infinity, the angle of refraction always tends to zero, and so refracted wave propagates along the normal to the slab's surface and consequently $|\mathbf{k}_{L(R)}|=k_{L(R)}=k_{L(R)_x}$. Thereby magneto-optic activity is only manifest in polar geometry, and to convert the propagation matrix (2.6) to the linear polarization representation we can use expression

$$\hat{P} = \hat{U}\hat{P}^{circ}\hat{U}^{-1}, \tag{2.7}$$

where $\hat{U}$ is the transformation matrix from circular polarization representation to linear polarization representation:[18]

$$\hat{U} = \begin{bmatrix} 1 & 0 & 1 & 0 \\ 0 & 1 & 0 & 1 \\ i & 0 & -i & 0 \\ 0 & i & 0 & -i \end{bmatrix}. \tag{2.8}$$

The final expression for transfer matrix of the magnetoactive slab is

$$\hat{D} = \hat{D}_{12} \times \hat{U} \times \hat{P}_2^{circ} \times \hat{U}^{-1} \times \hat{D}_{12}{}^{-1}. \tag{2.9}$$

Additional simplification in the limit (2.1) can be achieved by expanding exponents in the resulting transfer matrix into series by value $k_{L(R)}d$ and terminating the resulting series after second term. Such an approximation in the optics of thin films is also known as the ultrathin-film approximation.[17] Using this approximation, after tedious but straightforward calculations, we obtain the final expression for the transfer matrix of a single magnetoactive layer of infinitesimal thickness:

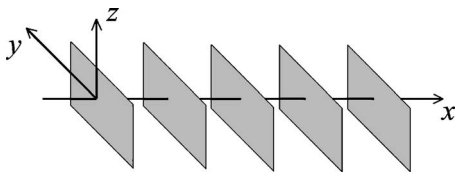

FIG. 2. Geometrical arrangement of a one-dimensional array of infinitesimal magnetoactive sheets.

$$\hat{D} = \begin{bmatrix} 1+i\frac{m}{2}\frac{k^2}{k_x} & i\frac{m}{2}\frac{k^2}{k_x} & \Delta\frac{k}{4} & \Delta\frac{k}{4} \\ -i\frac{m}{2}\frac{k^2}{k_x} & 1-i\frac{m}{2}\frac{k^2}{k_x} & -\Delta\frac{k}{4} & -\Delta\frac{k}{4} \\ -\Delta\frac{k}{4} & -\Delta\frac{k}{4} & 1+i\frac{m}{2}k_x & i\frac{m}{2}k_x \\ \Delta\frac{k}{4} & \Delta\frac{k}{4} & -i\frac{m}{2}k_x & 1-i\frac{m}{2}k_x \end{bmatrix}, \tag{2.10}$$

where values k and k_x are defined in the optically inactive medium, since components of wave vector and its modulus related to the magneto-optic medium were excluded using relation $k_1 n_1 = k_2 n_2$, and the redundant index was omitted.

From Eq. (2.10) we see that if the parameter of magneto-optic activity Δ is equal to zero, then the transfer matrix $\hat{D}$ block diagonalizes to two (2×2) matrixes for s and p polarizations separately and coincides with the transfer matrix given in Ref. 13. If Δ is not equal to zero, then the mixing of s and p polarizations appears during propagation through sheet, and simple separation of polarizations becomes impossible. Such coupling of the s- and p-polarized modes in some sense is very similar to those found in PC's infiltrated by liquid crystals in Refs. 6 and 7 and similarly originates from anisotropy that breaks the mirror symmetry of 2D PC. However, the nature of magnetoinduced anisotropy differs from the nature of ordinary anisotropy, resulting in difference of the s-p coupled eigenstates in MPC's and in PC's infiltrated by liquid crystals.

III. ONE-DIMENSIONAL MAGNETOACTIVE LATTICE

In this section we consider an infinite one-dimensional array of infinitesimal magnetoactive dielectric sheets described in the previous section. The array of sheets with period a is shown in Fig. 2. The electric field in the primitive cell region defined in the free space between the sheets labeled $n-1$ and n can be written as

$$\begin{pmatrix} E_s^+(\mathbf{r}) \\ E_s^-(\mathbf{r}) \\ E_p^+(\mathbf{r}) \\ E_p^-(\mathbf{r}) \end{pmatrix} = e^{ik_y y} \begin{pmatrix} e^{ik_x x} & 0 & 0 & 0 \\ 0 & e^{-ik_x x} & 0 & 0 \\ 0 & 0 & e^{ik_x x} & 0 \\ 0 & 0 & 0 & e^{-ik_x x} \end{pmatrix} \times \begin{pmatrix} E_s^+ \\ E_s^- \\ E_p^+ \\ E_p^- \end{pmatrix}_n \quad \text{for } (n-1)a < x < na, \quad (3.1)$$

where the time dependence $e^{-i\omega t}$ is understood in all fields. The lattice is isotropic in the yz plane, and we have again taken $k_z=0$. Vacuum wave-vector components k_x and k_y, which are perpendicular and parallel to sheets, are related by

$$k_x^2 + k_y^2 = k^2 = \omega^2/c^2. \quad (3.2)$$

The relations between the fields in adjacent primitive cells can be obtained with a transfer matrix $\hat{D}$. The resulting relation between the electric-field amplitudes in cells n and $n+1$ can be written as

$$\begin{bmatrix} E_s^+ \\ E_s^- \\ E_p^+ \\ E_p^- \end{bmatrix}_{n+1} = \begin{bmatrix} \exp(-ink_x a) & 0 & 0 & 0 \\ 0 & \exp(ink_x a) & 0 & 0 \\ 0 & 0 & \exp(-ink_x a) & 0 \\ 0 & 0 & 0 & \exp(ink_x a) \end{bmatrix} \times \begin{bmatrix} 1+i\frac{m}{2}\frac{k^2}{k_x} & i\frac{m}{2}\frac{k^2}{k_x} & \Delta\frac{k}{4} & \Delta\frac{k}{4} \\ -i\frac{m}{2}\frac{k^2}{k_x} & 1-i\frac{m}{2}\frac{k^2}{k_x} & -\Delta\frac{k}{4} & -\Delta\frac{k}{4} \\ -\Delta\frac{k}{4} & -\Delta\frac{k}{4} & 1+i\frac{m}{2}k_x & i\frac{m}{2}k_x \\ \Delta\frac{k}{4} & \Delta\frac{k}{4} & -i\frac{m}{2}k_x & 1-i\frac{m}{2}k_x \end{bmatrix} \times \begin{bmatrix} \exp(ink_x a) & 0 & 0 & 0 \\ 0 & \exp(-ink_x a) & 0 & 0 \\ 0 & 0 & \exp(ink_x a) & 0 \\ 0 & 0 & 0 & \exp(-ink_x a) \end{bmatrix} \times \begin{bmatrix} E_s^+ \\ E_s^- \\ E_p^+ \\ E_p^- \end{bmatrix}_n. \quad (3.3)$$

The relation between the electric-field amplitudes given in Eq. (3.3) is entirely derived from the properties of the electromagnetic field and the dielectric sheets, but these same field amplitudes are independently related by Bloch's theorem, which applies generally to all forms of excitation in a periodic structure. For the present system, Bloch's theorem takes the form

$$\begin{bmatrix} E_s^+(\mathbf{r}+\hat{\mathbf{x}}a) \\ E_s^-(\mathbf{r}+\hat{\mathbf{x}}a) \\ E_p^+(\mathbf{r}+\hat{\mathbf{x}}a) \\ E_p^-(\mathbf{r}+\hat{\mathbf{x}}a) \end{bmatrix}_{n+1} = \exp(i\mu_x a) \begin{bmatrix} E_s^+(\mathbf{r}) \\ E_s^-(\mathbf{r}) \\ E_p^+(\mathbf{r}) \\ E_p^-(\mathbf{r}) \end{bmatrix}_n, \quad (3.4)$$

where μ_x is the one-dimensional Bloch wave vector and the primitive-cell electric-field amplitudes are defined in Eq. (3.1).

The amplitudes in primitive cell $n+1$ are easily eliminated from Eqs. (3.3) and (3.4), and the resulting equation for the amplitudes in primitive cell n is written as

$$\begin{bmatrix} \left(1+i\frac{m}{2}\frac{k^2}{k_x}\right)e^{ik_xa}-e^{i\mu_xa} & i\frac{m}{2}\frac{k^2}{k_x}e^{-i(2n-1)k_xa} & \Delta\frac{k}{4}e^{ik_xa} & \Delta\frac{k}{4}e^{-i(2n-1)k_xa} \\ -i\frac{m}{2}\frac{k^2}{k_x}e^{i(2n-1)k_xa} & \left(1-i\frac{m}{2}\frac{k^2}{k_x}\right)e^{-ik_xa}-e^{i\mu_xa} & -\Delta\frac{k}{4}e^{i(2n-1)k_xa} & -\Delta\frac{k}{4}e^{-ik_xa} \\ -\Delta\frac{k}{4}e^{ik_xa} & -\Delta\frac{k}{4}e^{-i(2n-1)k_xa} & \left(1+i\frac{m}{2}k_x\right)e^{ik_xa}-e^{i\mu_xa} & i\frac{m}{2}k_xe^{-i(2n-1)k_xa} \\ \Delta\frac{k}{4}e^{i(2n-1)k_xa} & \Delta\frac{k}{4}e^{-ik_xa} & -i\frac{m}{2}k_xe^{i(2n-1)k_xa} & \left(1-i\frac{m}{2}k_x\right)e^{-ik_xa}-e^{i\mu_xa} \end{bmatrix} \times \begin{bmatrix} E_s^+ \\ E_s^- \\ E_p^+ \\ E_p^- \end{bmatrix} = 0. \tag{3.5}$$

The determinant of the 4×4 matrix essentially identifies the Bloch exponent $\exp(i\mu_xa)$ as an eigenvalue of the transfer matrix, and the multiplied-out determinant can be written as

$$\left(\cos(\mu_xa)-\cos(k_xa)+\frac{m}{2}\frac{k^2}{k_x}\sin(k_xa)\right)\left(\cos(\mu_xa)-\cos(k_xa)+\frac{m}{2}k_x\sin(k_xa)\right)-\Delta^2\frac{k^2}{8}\sin(k_xa)=0. \tag{3.6}$$

This expression determines the dispersion relation—that is, the dependence of the frequency on the Bloch wave vector μ_x for a given value of the transfer wave-vector component k_y—for the propagation of electromagnetic waves through the one-dimensional array of magnetoactive dielectric sheets.

Solving Eq. (3.6) as a quadratic equation for $\cos(\mu_xa)$ we obtain the dispersion relations

$$\cos(\mu_xa)=\cos(k_xa)-\left\{\frac{m}{4}\left(\frac{k^2}{k_x}+k_x\right)\pm\sqrt{\left[\frac{m}{4}\left(\frac{k^2}{k_x}-k_x\right)\right]^2+\left(\Delta\frac{k}{4}\right)^2}\right\}\sin(k_xa), \tag{3.7}$$

where these expressions yield the two dispersion relations for s and p polarizations obtained in Ref. 5 if we assume the parameter of the magneto-optic activity Δ to be equal to zero:

$$\cos(\mu_xa)=\cos(k_xa)-\frac{m}{2}\frac{k^2}{k_x}\sin(k_xa),$$

$$\cos(\mu_xa)=\cos(k_xa)-\frac{m}{2}k_x\sin(k_xa). \tag{3.8}$$

Consequently, because of the small natural values of the magneto-optic parameter Δ, a direct correspondence between branches of spectra for electromagnetic modes in magnetic and nonmagnetic lattices can be ascertained, whereas their polarization states can be far different. Therefore we use the notation quasi-s and quasi-p to designate the polarization state of solutions with the upper and lower signs in the second term of the right-hand side of Eq. (3.7).

IV. TWO-DIMENSIONAL MAGNETOACTIVE LATTICE

In this section we consider MPC's formed from infinite lattices of two identical arrays of infinitesimal magnetoactive dielectric sheets at right angles. The x and y axes are taken as normals to the sheets, which have indefinite extents in the z axis direction (Fig. 3). The photonic band structure in MPC's formed in this way is studied and alteration of spectra is analyzed.

The calculations presented here assume propagation parallel to the xy plane with wave vector $\mathbf{k}=(k_x,k_y)$ whose components satisfy Eq. (3.2). The corresponding wave-vector space is thus two dimensional. The Bloch wave vector is denoted as $\boldsymbol{\mu}=(\mu_x,\mu_y)$, and the associated two-dimensional Brillouin zone of the lattice covers the range

$$-\pi/a<\mu_x,\quad \mu_y<\pi/a. \tag{4.1}$$

One quadrant of the Brillouin zone with conventional notation for its high-symmetry points is shown in Fig. 4.

In a two-dimensional lattice, the procedure introduced for a one-dimensional lattice can be applied separately to adjacent cells in the x and y directions. Since the field in each cell is described by eight-component vectors of field amplitudes, they must correspond to quasi-s- and quasi-p-polarized waves propagating in the positive and negative directions of the x and y axes, respectively. However, the four components that describe propagation in the x direction

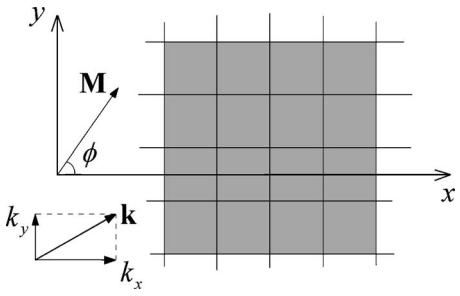

FIG. 3. Cross section of a two-dimensional MPC composed from sheets of infinitesimal thickness in the xy plane.

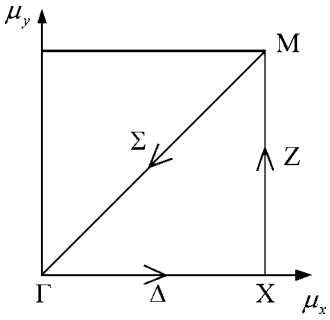

FIG. 4. Brillouin zone of a square two-dimensional lattice showing the notation of symmetry points and directions.

do not couple to the four components that describe propagation in the y direction. As a result, the associated 8×8 transfer matrix block diagonalizes to two 4×4 matrices of the form shown in Eq. (3.3); the connections are the same as found for the one-dimensional lattice. Bloch's theorem also separates into two relations equivalent to Eq. (3.4). Therefore, the two-dimensional calculation results in a pair of relations similar to Eq. (3.7):

$$\cos(\mu_x a) = \cos(k_x a) - \left\{ \frac{m}{4}\left(\frac{k^2}{k_x} + k_x\right) \pm \sqrt{\left[\frac{m}{4}\left(\frac{k^2}{k_x} - k_x\right)\right]^2 + \left(\Delta_x \frac{k}{4}\right)^2} \right\} \sin(k_x a),$$

$$\cos(\mu_y a) = \cos(k_y a) - \left\{ \frac{m}{4}\left(\frac{k^2}{k_y} + k_y\right) \pm \sqrt{\left[\frac{m}{4}\left(\frac{k^2}{k_y} - k_y\right)\right]^2 + \left(\Delta_y \frac{k}{4}\right)^2} \right\} \sin(k_y a). \tag{4.2}$$

Here, the upper sign corresponds to the quasi-s polarization, the lower one to the quasi-p polarization, and Δ_x and Δ_y are parameters of a magnetic activity for arrays of sheets arranged along the x and y axes, respectively. Because the wave inside the dielectric sheet with infinite permittivity always propagates along the normal to its surface, we conclude that values Δ_x and Δ_y can be represented as

$$\Delta_x = \Delta\cos\varphi, \quad \Delta_y = \Delta\sin\varphi, \tag{4.3}$$

where φ is the angle between the directions of the magnetization $\mathbf{M}$ and the x axis (Fig. 3).

System (4.2) represents the exact dispersion relations for two-dimensional MPC's. However, since it cannot be solved analytically because of its transcendental structure, we used numerical methods to solve it.

Consider the case when external field is applied to the x direction—i.e., $\Delta_x=\Delta$ and $\Delta_y=0$. To distinguish the dispersion curves in the figures, in our numerical calculations we used a rather large value of magneto-optic parameter $\Delta=0.1m$, whereas the parameter m was taken to be equal to double lattice constant ($m=2a$). The dispersion curves for the quasi-p-polarized wave for magnetic and nonmagnetic cases are plotted in Fig. 5. To show the difference between these two cases, the vicinities of Γ and M points for the second and third branches of the spectrum are plotted in Figs. 6 and 7. It can be seen that because of the influence of external magnetic fields, which reduces symmetry of the structure under investigation, splitting of "energy" levels in the ΓM (Σ) direction appears. This effect is the optical counterpart of the Zeeman effect, when an external magnetic field causes electron energy level splitting.

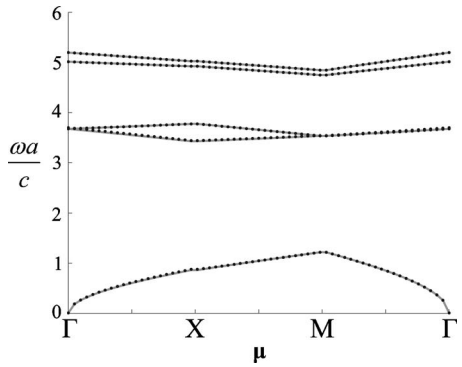

FIG. 5. Dispersion relation ω vs the Bloch wave vector μ for p-polarized modes. Solid gray lines show the nonmagnetic case; black dotted lines show the magnetic case (magnetic field applied to the x direction).

Because of symmetry breaking, the irreducible zone becomes twice as large in the magnetized MPC, and we must study additional paths in the Brillouin zone, which are obtained by reflection of the $\Gamma\rightarrow X(\Delta)$ and $X\rightarrow M(Z)$ paths about the $\Gamma M(\Sigma)$ direction (Fig. 4). However, it is obvious that such additional information can be obtained by investigation of the same paths for the external magnetic field applied to the y direction.

It is illustrative to display the contour diagrams to present the behavior of electromagnetic wave modes inside of the allowed bands. Several are presented in Figs. 8–10 for the first, second, and third branches of the spectrum, respectively. It is worthy to note that the modes of the third band

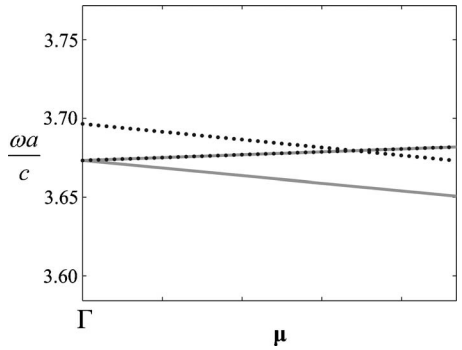

FIG. 6. Dispersion relation ω vs the Bloch wave vector μ for p-polarized modes in vicinity of the Γ point. Solid gray lines show the nonmagnetic case; black dotted lines show the magnetic case (magnetic field applied to the x direction).

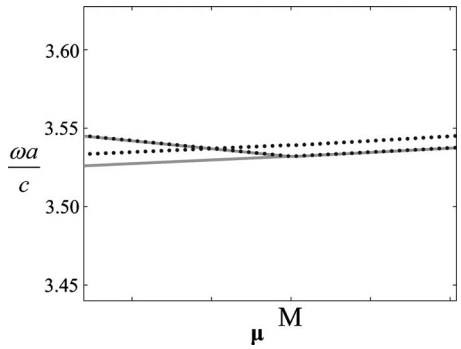

FIG. 7. Dispersion relation ω vs the Bloch wave vector μ for p-polarized modes in vicinity of the M point. Solid gray lines show the nonmagnetic case; black dotted lines show the magnetic case (magnetic field applied to the x direction).

are altered by magnetization in a considerably different way than the modes of the first and second bands. Indeed, equal-frequency contours for the third band change their structure mainly in the μ_y direction, whereas the modes of the first and second bands change their structure mainly in the μ_x direction. Such behavior shows that some modes "feel" influence of the optical activity in the direction orthogonal to external magnetic field.

One can also note that an external magnetic field affects modes closest to the band edges more intensively. It reflects the well-known fact of the abnormally slow group velocity of electromagnetic waves at the band edges of the spectrum. This increases the interaction time of the electromagnetic waves with the structure under investigation and, as a consequence, causes enhancement of all physical phenomena.

If an external magnetic field is applied to the MPC in the xy direction ($\varphi=\pi/4$), then it does not break the symmetry of the crystal and the band structure maintains the same view, as in the nonmagnetic case. However, the second and third branches simultaneously shift in the high-frequency region. The contour diagrams again show the strongest sensitivity of dispersion near band edges.

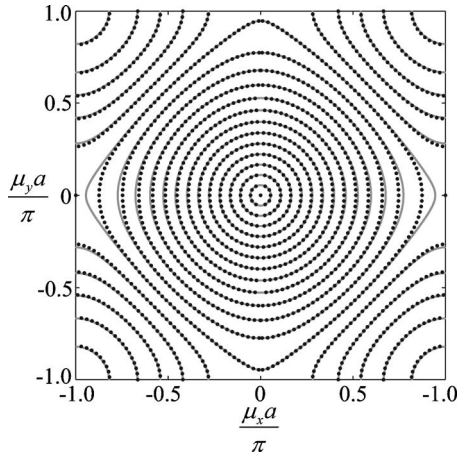

FIG. 8. Constant-frequency contours ($\omega a/c=0,0.1,0.2,\ldots,1.8$) for the first band of p-polarized modes. Solid gray lines show the nonmagnetic case; black dotted lines show the magnetic case (magnetic field applied to the x direction).

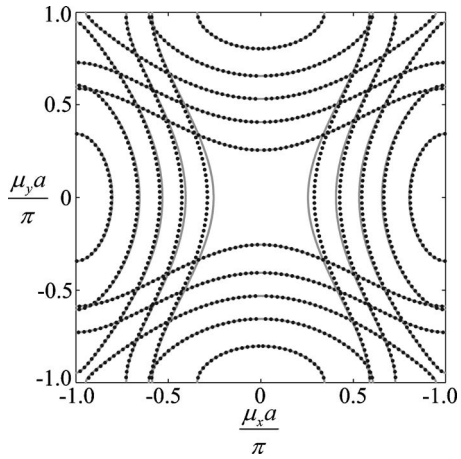

FIG. 9. Constant-frequency contours ($\omega a/c=3.0,3.1,3.2,\ldots,3.6$) for the second band of p-polarized modes. Solid gray lines show the nonmagnetic case; black dotted lines show the magnetic case (magnetic field applied to the x direction).

By analogy, the band structure for quasi-s polarization can be studied, but because it changes in a manner similar to quasi-p polarization we do not consider it here.

Eigenstates of MPC's, in general, differ from eigenstates of isotropic photonic crystals. It is well known that eigenstates of a one-dimensional MPC for normal incidence are circularly polarized Bloch waves.[17] For the structure under investigation, this feature remains valid for the ΓX direction. This can be proven by transformation of the transfer matrix (2.10) into circular polarization representation:

$$\hat{D}^{circ} = \hat{U}^{-1}\hat{D}\hat{U}. \tag{4.4}$$

In this representation, the transfer matrix takes a block-diagonal form for the ΓX direction, which reflects the existence of two independent left- and right-circularly polarized modes with the Bloch wave vector oriented in the same ΓX direction. It shows that the quasi-s- and quasi-p-polarized

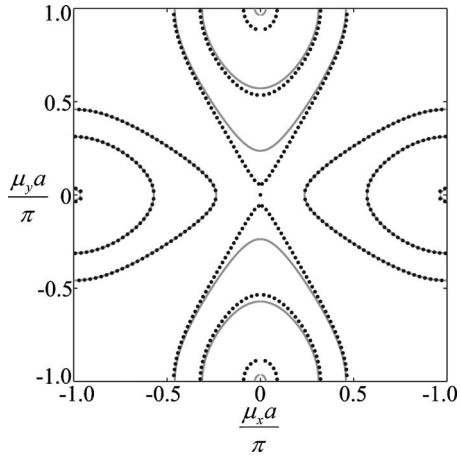

FIG. 10. Constant-frequency contours ($\omega a/c=3.7,3.8,3.9$) for the third band of p-polarized modes. Solid gray lines show the nonmagnetic case; black dotted lines show the magnetic case (magnetic field applied to the x direction).

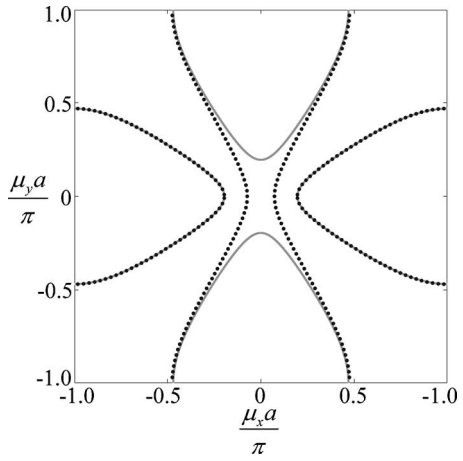

FIG. 11. Constant-frequency contours for the electromagnetic mode ($\omega a/c=3.69$) that exhibits bistable behavior. Solid gray lines show the nonmagnetic case; black dotted lines show the magnetic case (magnetic field applied to the x direction).

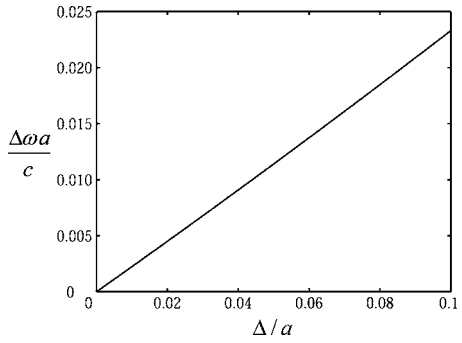

FIG. 12. Dependence of the frequency range, where electromagnetic modes exhibit bistable behavior, vs the parameter of magneto-optic activity.

eigenmodes of MPC's can be far different from linearly polarized eigenmodes of the nonmagnetic PC's. Similar to results for the uniform magneto-optic material, for the ΓX direction in the MPC under study, magnetization removes the degeneracy between the left- and right-polarized modes, changing the absolute values of their Block wave vectors. In such a case the effective Faraday rotatory power of a MPC can be evaluated as the difference of the modulus of Bloch wave vectors for the left- and right-polarized modes.[12]

For directions different from the ΓX direction, the transfer matrix (2.10) cannot be brought to block-diagonal form by transformation to the circular representation. The latter fact shows that MPC eigenstates for these directions are not purely circularly polarized modes. Their polarization state can be represented as linear combinations of linear s and p polarizations, which for the ΓX direction yields left- and right-circular polarizations and partially circularly polarization for other directions. Since directions of Bloch wave vectors for such quasi-s- and quasi-p-polarized states of the same frequency do not coincide, it causes an effect analogous to the linear magnetic birefringence.[12]

The theoretical model under investigation predicts another unusual behavior in the vicinity of degeneracy at the Γ point. Modes of a certain frequency range near the degeneracy, because of splitting of the degenerate energy surfaces in the external magnetic field, exhibit profound alteration of dispersion. An example of such behavior for a frequency near degeneracy is shown in Fig. 11. It can be seen that the mode of the third branch of the spectrum changes its dispersion to the dispersions peculiar to the second branch. Moreover, alteration of the dispersion exhibits discontinuous dependence on the parameter of magneto-optic activity Δ and does not depend on its absolute value. The latter circumscribes only a frequency range where this effect appears (Fig. 12). That is, for any small absolute value of the parameter Δ, one can find a frequency range in the vicinity of degeneracy where such bistable behavior occurs.

It is obvious that alteration of dispersion will simultaneously cause a discontinuous change of the propagation direction of the electromagnetic wave, since the latter is completely defined by constant-frequency contours.[19] As can be seen from analysis of contours in Fig. 11, for certain Bloch wave vectors within Brillouin zone, the deflection angle of the wave propagation direction can reach 90°. At the same time, because of proximity to the Γ point (or the ΓX direction), polarization of the propagating electromagnetic wave will be changed from linear to circular.

We now consider generalization of the theory presented here to the case of Voigt (Cotton-Mouton) geometry—i.e., when the external magnetic field applied to the direction normal to the plane of 2D MPC. As seen in Fig. 3, this direction coincides with the direction of the z axis. Since the direction of the external magnetic field is orthogonal to the wave vector $\mathbf{k}$, the influence of the Faraday effect disappears and the Cotton-Mouton effect assumes the main role. It is well known that the Cotton-Mouton effect leads to the appearance of uniaxial anisotropy.[20] Because of the coincidence of the axis of anisotropy and direction the z axis, only s polarization is affected by an external magnetic field. Moreover, because of the absence of mixing between s and p polarizations, the dispersion relation for s polarization can be easily obtained by substitution in the first expression of Eq. (3.8):

$$m \to m_{\perp} = \varepsilon_{\perp} d = n_{\perp}{}^2 d, \tag{4.5}$$

where $\perp$ denotes value of the parameter in the direction orthogonal to the plane of the MPC (xy plane). The dispersion relation for p polarization remains unchanged because the external magnetic field does not affect the permittivity for directions parallel to the MPC plane. Finally, considering the weakness of the Cotton-Mouton effect, we conclude that in the Voigt (Cotton-Mouton) geometry, the band structure for s polarization only changes insignificantly, whereas the band structure for p polarization remains unchanged.

V. CONCLUSION

We investigated the optical properties of a 2D MPC which represents a square lattice of magnetoactive dielectric sheets in the limit where the sheet thickness tends to zero as its relative permittivity tends to infinity. Dispersion relations for this structure were obtained in exact form.

The band structure of the model 2D MPC was analyzed for two geometries: Faraday and Voigt. It was shown that for

the Faraday geometry, magneto-optic activity of the sheets, reduces crystal symmetry resulting in the splitting of degenerate energy levels in the presence of an external magnetic field. For the Voigt geometry magneto-optic activity does not affect the band structure for *p* polarization, whereas changes in band structure for *s* polarization are negligible.

For Faraday geometry, despite the weakness of magneto-optic activity, a strong sensitivity of the dispersion of electromagnetic modes was found in the vicinity of the band edges, reflecting an enhancement of the interaction of electromagnetic waves with a medium that constituted a MPC.

It is also shown that in the vicinity of degeneracy, electromagnetic eigenmodes of MPC exhibit bistable behavior and discontinuously change their dispersion, causing a discontinuous alteration of the refraction angle in the MPC up to 90° when an external magnetic field is applied. At the same time, the polarization of the eigenmodes changes from linear to circular which causes the selective transmittance or reflectance of circularly polarized subcomponents of the incident light. This effect increases the importance of MPC's for applications because of the possibility of ultrafast optical tuning of refraction and/or polarization state of electromagnetic waves by magnetization. It is especially expected to be important for such promising and challenging structures as superlenses and superprisms, which have PC's in their basis and offer the possibility of propagation control and, in the case of MPC's, control of the polarization state of electromagnetic waves as well.

*Permanent address: A.F. Ioffe Physico-Technical Institute, 194021 St. Petersburg, Russia.

[1] E. Yablonovitch, Phys. Rev. Lett. **58**, 2059 (1987); S. John, *ibid.* **58**, 2486 (1987).
[2] J. D. Joannopoulos, R. D. Meade, and J. N. Winn, *Photonic Crystals* (Princeton University Press, Princeton, 1995); K. Sakoda, *Optical Properties of Photonic Crystals* (Springer, Berlin, 2001).
[3] A. Figotin, Y. A. Godin, and I. Vitebsky, Phys. Rev. B **57**, 2841 (1998).
[4] K. Busch and S. John, Phys. Rev. Lett. **83**, 967 (1999).
[5] H. Takeda and K. Yoshino, Phys. Rev. E **67**, 056607 (2003).
[6] H. Takeda and K. Yoshino, Phys. Rev. E **67**, 056612 (2003).
[7] H. Takeda and K. Yoshino, Phys. Rev. E **68**, 046602 (2003).
[8] Z.-Y. Li, J. Wang, and B.-Y. Gu, Phys. Rev. B **58**, 3721 (1998); H. Chen, W. Zhang, Z. Wang, and N. Ming, J. Phys.: Condens. Matter **16**, 165 (2004).
[9] M. Inoue *et al.*, J. Appl. Phys. **85**, 5768 (1999).
[10] A. Figotin and I. Vitebsky, Phys. Rev. E **63**, 066609 (2001).
[11] A. Figotin and I. Vitebskiy, Phys. Rev. B **67**, 165210 (2003).
[12] A. K. Zvezdin and V. I. Belotelov, Eur. Phys. J. B **37**, 479 (2004).
[13] T. J. Shepherd and P. J. Roberts, Phys. Rev. E **51**, 5158 (1995); T. J. Shepherd, P. J. Roberts, and R. Loudon, *ibid.* **55**, 6024 (1997).
[14] A. Figotin and Y. A. Godin, J. Appl. Math. **61**, 1959 (2001).
[15] F. Seitz, *The Modern Theory of Solids* (McGraw-Hill, New York, 1940).
[16] J. M. Ziman, *Models of Disorder* (Cambridge University Press, Cambridge, England, 1979).
[17] S. Visnovsky, K. Postava, and T. Yamaguchi, Opt. Express **9**, 158 (2001).
[18] P. Yeh, *Optical Waves in Layered Media* (Wiley Interscience, New York, 1988).
[19] H. Kosaka, T. Kawashima, A. Tomita, M. Notomi, T. Tamamura, T. Sato, and S. Kawakami, Phys. Rev. B **58**, R10096 (1998).
[20] L. D. Landau and E. M. Lifschitz, *Electrodynamics of Continuous Media* (Pergamon Press, Oxford, 1984).